ELSEVIER

COMMENTARY

Structure-Based Drug Design of Non-nucleoside Inhibitors for Wild-Type and Drug-Resistant HIV Reverse Transcriptase

Chen Mao,*† Elise A. Sudbeck,*† T. K. Venkatachalam*‡ and Fatih M. Uckun*§∥
DRUG DISCOVERY PROGRAM, AND DEPARTMENTS OF †STRUCTURAL BIOLOGY, ‡CHEMISTRY, AND §VIROLOGY, HUGHES INSTITUTE, ST. PAUL, MN 55113, U.S.A.

ABSTRACT. The generation of anti-HIV agents using structure-based drug design methods has yielded a number of promising non-nucleoside inhibitors (NNIs) of HIV reverse transcriptase (RT). Recent successes in identifying potent NNIs are reviewed with an emphasis on the recent trend of utilizing a computer model of HIV RT to identify space in the NNI binding pocket that can be exploited by carefully chosen functional groups predicted to interact favorably with binding pocket residues. The NNI binding pocket model was used to design potent NNIs against both wild-type RT and drug-resistant RT mutants. Molecular modeling and score functions were used to analyze how drug-resistant mutations would change the RT binding pocket shape, volume, and chemical make-up, and how these changes could affect inhibitor binding. Modeling studies revealed that for an NNI of HIV RT to be active against RT mutants such as the especially problematic Y181C RT mutant, the following features are required: (a) the inhibitor should be highly potent against wild-type RT and therefore capable of tolerating a considerable activity loss against RT mutants (i.e. a picomolar-level inhibitor against wild-type RT may still be effective against RT mutants at nanomolar concentrations), (b) the inhibitor should maximize the occupancy in the Wing 2 region of the NNI binding site of RT, and (c) the inhibitor should contain functional groups that provide favorable chemical interactions with Wing 2 residues of wild-type as well as mutant RT. Our rationally designed NNI compounds HI-236, HI-240, HI-244, HI-253, HI-443, and HI-445 combine these three features and outperform other anti-HIV agents examined.   BIOCHEM PHARMACOL **60**;9: 1251–1265, 2000. © 2000 Elsevier Science Inc.

KEY WORDS. HIV; reverse transcriptase; non-nucleoside inhibitor; drug resistance; drug design; molecular modeling

One of the main targets in contemporary drug discovery efforts against HIV-1¶ is RT, a vital enzyme that is responsible for the reverse transcription of retroviral RNA to proviral DNA [1–3]. The three categories of antiretroviral agents currently in use include nucleoside analogs (such as AZT), protease inhibitors (such as nelfinavir), and the recently introduced non-nucleoside RT inhibitors (NNIs or NNRTIs) such as nevirapine, delavirdine, and efavirenz. Combination therapies may be a significant factor in the dramatic decrease in deaths from AIDS [4]. The most commonly used combinations include two nucleoside analogs with or without a protease inhibitor [5]. In recent years, structure-based drug design has played an increasingly important role in the development of useful drugs, as demonstrated by the success of HIV protease

∥ Corresponding author: Dr. Fatih M. Uckun, Parker Hughes Institute, 2665 Long Lake Road, St. Paul, MN 55113. Tel. (651) 697-9228; FAX (651) 697-1042; E-mail: Fatih_Uckun@ih.org

¶ *Abbreviations:* HIV-1, human immunodeficiency virus type 1; NNI, non-nucleoside inhibitor; NNRTI, non-nucleoside reverse transcriptase inhibitor; RT, reverse transcriptase; PBMC, human peripheral blood mononuclear cells; MDR, multiple drug-resistant strain; LUDI, empirical scoring function developed by H. Bohm; BHAP, delavirdine [bis(heteroaryl)piperazine]; DABO, dihydroalkoxybenzyloxopyrimidine; S-DABO, dihydroalkoxybenzylthiopyrimidine; TIBO, tetrahydroimidazo-(4,5,1-*j*,*k*)(1,4)-benzodiazepin-2(1*H*)-thione; TSAO, 2′,5′-bis-O-(*tert*-butyldimethylsilyl)-3′-spiro-5′-(4″-amino-1″,2″-oxathiole-2″,2″-dioxide)pyrimidine; PETT, phenethylthiazolylthiourea; TNK, 6-benzyl-1-benzyloxymethyl uracil; HEPT, 1-[(2-hydroxyethoxy)methyl]-6-(phenylthio)thymine; MKC-442, a HEPT derivative; APA and α-APA, α-anilinophenylacetamide; dNTP, deoxynucleotide triphosphate; AZT, 3′-azido-3′-deoxythymidine; ddC, 2′,3′-dideoxycytidine; ddI, 2′,3′-dideoxyinosine; HTLV, human T-lymphotropic virus; 3TC, (-)-2′-deoxy-3′-thiacytidine; HI-231, N-[2-(4-nitrophenyl)ethyl]-N′-[2-(5-bromopyridyl)]-thiourea; HI-236, N-[2-(2,5-dimethoxyphenylethyl)]-N′-[2-(5-bromopyridyl)]-thiourea; HI-238, N-[2-(4-methoxyphenyl)ethyl]-N′-[2-(5-bromopyridyl)]-thiourea;

HI-240,   N-[2-(2-fluorophenethyl)]-N′-[2-(5-bromopyridyl)]-thiourea;
HI-241,   N-[2-(3-fluorophenyl)ethyl]-N′-[2-(5-bromopyridyl)]-thiourea;
HI-242,   N-[2-(4-fluorophenyl)ethyl]-N′-[2-(5-bromopyridyl)]-thiourea;
HI-243,   N-[2-(4-bromophenyl)ethyl]-N′-[2-(5-bromopyridyl)]-thiourea;
HI-244,   N-[2-(4-methylphenyl)ethyl]-N′-[2-(5-bromopyridyl)]-thiourea;
HI-253,   N-[2-(2-chlorophenethyl)]-N′-[2-(5-bromopyridyl)]-thiourea;
HI-255,   N-[2-(4-chlorophenyl)ethyl]-N′-[2-(5-bromopyridyl)]-thiourea;
HI-256, N-[2-(4-hydroxyphenyl)ethyl]-N′-[2-(5-bromopyridyl)]-thiourea;
HI-275, N-[2-phenylethyl]-N′-[2-(5-bromopyridyl)]-thiourea; HI-280, 5-isopropyl-2-[(methylthiomethyl)thio]-6-(benzyl)-pyrimidin-4-(1*H*)-one; HI-281, 5-isopropyl-2-[(methylthiomethyl)thio]-6-(3,5-dimethylbenzyl)-pyrimidin-4-(1*H*)-one; HI-346, N-[2-(1-cyclohexenyl)ethyl]-N′-[2-(5-bromopyridyl)]-thiourea; HI-347, N-[2-(1-cyclohexenyl)ethyl]-N′-[2-(5-trifluoromethylpyridyl)]-thiourea; HI-443, N-[2-(2-thiophenyl)ethyl] N′-[2-(5-bromopyridyl)]-thiourea; and HI-445, N-[2-(1-cyclohexenyl)ethyl] N′-[2-(5-chloropyridyl)]-thiourea.

Nevirapine   Delavirdine   Efavirenz   PETT
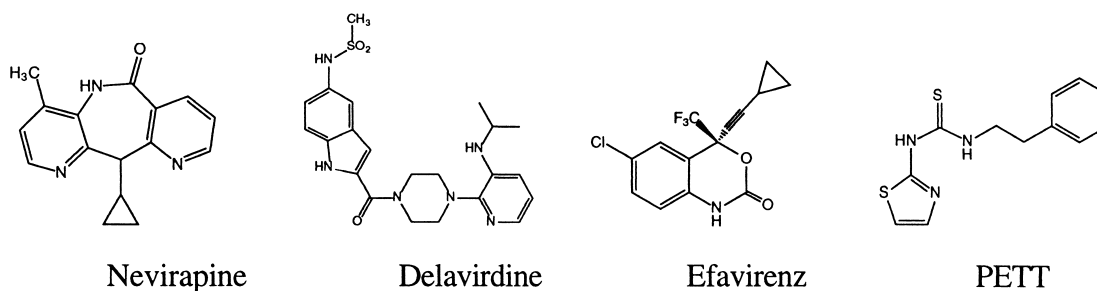
STRUCTURE 1.

inhibitor designs [6]. Nevirapine is currently the only NNI compound that has been used in combination with AZT and/or protease inhibitors for the treatment of HIV. A new series of effective drug combinations most likely will involve other NNIs in combination with nucleoside and protease inhibitors as a triple-action regimen to combat the growing problem of drug resistance encountered in single-drug treatment strategies. The high and erroneous replication rate of the virus unfortunately leads to genetic variants, especially when selective pressure is introduced in the form of drug treatment [7]. These mutant viral strains are resistant to the previously used anti-HIV agents. Switching agents or using combination therapies may decrease or delay resistance, but because viral replication is not completely suppressed in single-drug treatment strategies or even with a dual drug combination, drug-resistant viral strains ultimately emerge [8].

Three NNIs or NNRTIs of HIV RT that have been approved by the U.S. Food and Drug Administration for licensing and sale in the United States are nevirapine (a dipyridodiazepinone derivative) [9], delavirdine (a BHAP derivative, BHAP U-90152) [10–12], and efavirenz [13]. Other promising new NNIs that have been developed to inhibit HIV RT include DABO derivatives [14–18], HEPT derivatives [16, 19–21], TIBO derivatives [22], TSAO derivatives [23, 24], oxathiin carboxanilide derivatives [25–27], quinoxaline derivatives [28, 29], thiadiazole derivatives [30], and PETT derivatives [31–34].

MOLECULAR MECHANISM OF NNI INHIBITION AND DRUG RESISTANCE

Crystal structures, combined with biochemical data, have revealed a molecular mechanism for the polymerase activity of RT [35–38]. First, RT binds a primer–template between its "thumb" and "fingers" domains (Fig. 1). Upon binding with the incoming nucleotide triphosphate and magnesium in the catalytic site, which is marked by three aspartic residues, D110, D185, and D186, the "fingers" domain goes through a conformational change, moving closer to the catalytic site. Together with the aspartic residues, the Lys65 and Arg72 residues on the fingers domain form a tight-binding site for the correct nucleotide triphosphate, which is base-paired with template nucleotides to ensure replication fidelity. Through a nucleophilic in-line-attack two-metal-ion catalytic mechanism [39], the appropriate nucleotide is incorporated into the growing double strand, which
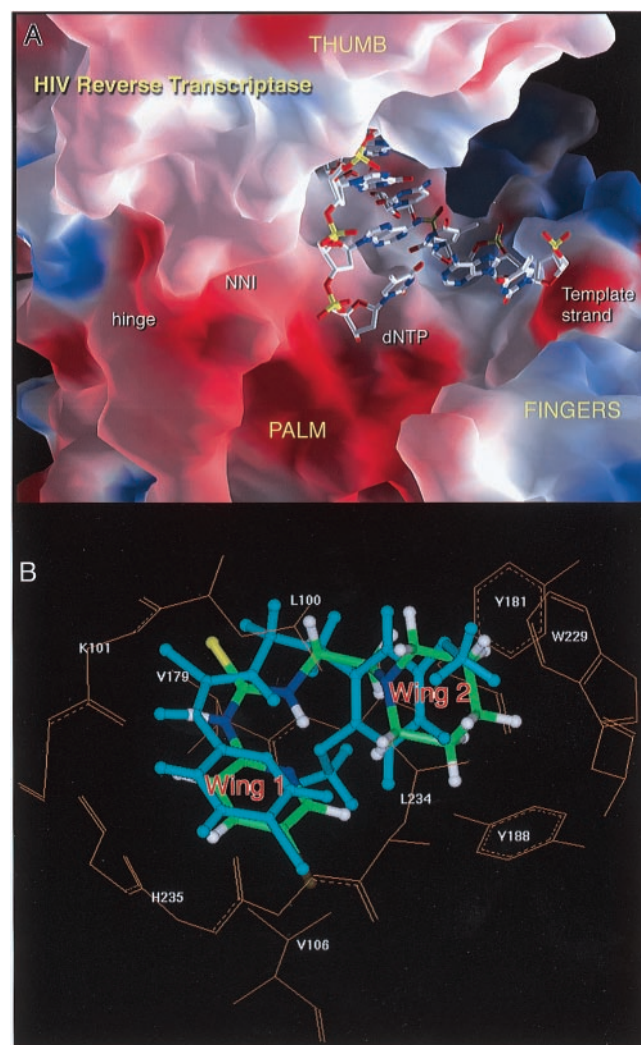

FIG. 1. (A) Model of HIV-1 RT active site, derived primarily from two crystal structures: HIV-1 RT (PDB access code 1hni) and HIV-1 RT with DNA fragment (PDB access code 1hmi). The binding site for NNIs is labeled NNI. The site for nucleoside inhibitors is labeled dNTP, which includes the 3′ terminus of DNA. Features describing the geometry of the binding region include the thumb, palm, fingers, and hinge region of RT. (B) Models of the compound N-[2-(1-piperidinoethyl)]-N′-[2-(5-bromopyridyl)]-thiourea (color coded by atom type) and compound N-[2-(2,5-dimethoxyphenylethyl)]-N′-[2-(5-bromopyridyl)]-thiourea (in blue) (HI-236) in the NNI binding site of HIV RT, positioned by a docking procedure. Wing 1 and Wing 2 represent two different regions of the NNI binding site.

then is translocated by one nucleotide-pair spacing and is ready for the next round of nucleotide incorporation. Therefore, nucleoside analogs (inhibitors) such as AZT, which is activated to AZT triphosphate *in vivo,* will be incorporated into the double strand by mistake and would terminate the nucleotide incorporation process. Unlike nucleoside analogs, NNIs bind to an allosteric site of HIV-1 RT [12, 22, 40–44], which is approximately 10 Å away from the catalytic site. NNI binding induces rotamer conformational changes in some residues (Y181 and Y188) and makes the thumb region more rigid. Both events consequently would alter the substrate binding mode and/or affect the translocation of the double strand, both of which are probably critical for the polymerase function, thereby leading to a noncompetitive inhibition of the enzyme [22, 40–44].

There is evidence that genetic variants of HIV containing a single mutation and double mutations exist in therapy-naive HIV-infected patients [45]. Thus, antiviral regimens containing nucleoside analogs or NNIs rapidly fail because of breakthrough replication of pre-existing resistant variants. The nucleoside analog inhibitors in clinical use are modified at the 3′ position: AZT has a 3′-azido group, whereas other drugs (ddC, 3TC, ddI) have no 3′ substituents. Based on the crystal structure of the RT ternary complex with duplex DNA and dNTP [35], the point mutations found in nucleoside-resistant strains (K65R, K70R, L74V, Q151M, M184I/V, and T215Y/F) are all in the neighborhood of the incoming nucleotide, whereas many of the reinforcing changes are in a more distant region. The aforementioned are the primary mutations that affect the position, stability, or reactivity of the bound analog itself, or, additionally, the templating base or primer terminus. A few of the RT mutations conferring resistance to the dideoxy class of inhibitors (including 3TC) are located close to one side of the pocket where the 3′ hydroxy group of dNTP binds, whereas some AZT-resistance mutations occur on the other side of the 3′ binding pocket.

In contrast, the mechanism underlying NNI resistance appears to be straightforward. Most mutations conferring resistance to NNIs are directly in contact with the NNI molecule, and thus are associated with changes in the binding of NNIs to RT (Fig. 2). For example, primary mutations associated with resistance to nevirapine involve residues K103, V106, V108, Y181, Y188, L100, and G190, which have van der Waals contact with the inhibitor. Mutations of these residues lead to the weakening of the inhibitor binding to RT. Delavirdine is more potent than nevirapine against wild-type RT and is less effective against RT with primary mutations K103N or Y181C. Efavirenz is less effective against RT with the primary mutation K103N.

The development of NNIs with high potency could provide a practical solution to the drug-resistance problem [48]. In the past decade, many classes of NNIs were discovered, mostly by chance [49, 50], and more recently, structure-based drug design has played an increasingly important role in the identification of highly potent NNIs. Our emphasis here will be on the more recent structure-based drug design efforts against HIV.
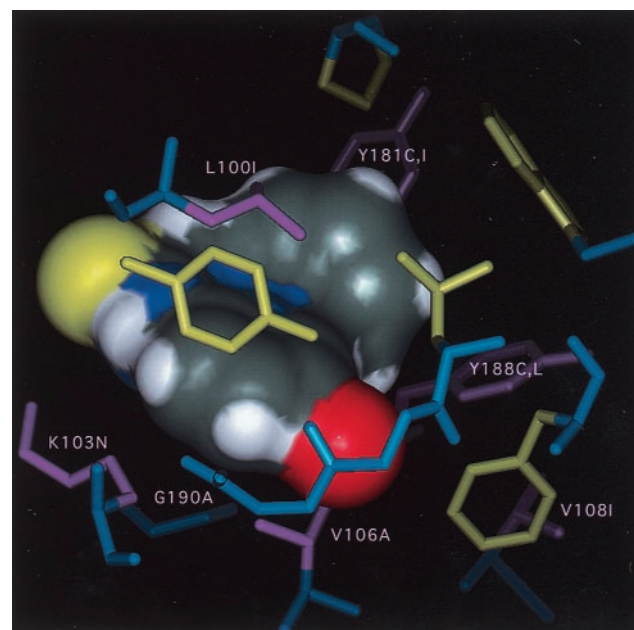

FIG. 2. Connolly surface [46] representation of compound HI-240 in the NNI binding site of HIV RT. The molecular surface areas associated with hydrogen atoms are colored in white. Other surface colors: nitrogen = blue, bromine = red, sulfur = yellow, and carbon = gray. The binding residues are shown in stick models. The main chains of these residues are colored in blue, and the side-chains of the residues that are mutated in NNI-resistant mutant strains are colored in pink and labeled (prepared using InsightII) [47]. The mutations reported to be resistant to nevirapine, delavirdine, or efavirenz are shown [45]. However, recent studies propose that any single mutant containing these mutations is unlikely to be selected in the presence of HI-240 due to its high potency.

STRUCTURAL INFORMATION AND COMPOSITE RT NNI BINDING POCKET MODEL

Rational drug design is most effective when detailed structural information about the protein–inhibitor complex is available. A number of crystal structures of RT complexed with NNIs have been reported (including α-APA, TIBO, nevirapine, and HEPT derivatives) [22, 40–44, 51, 52], and such structural information provides the basis for further derivatization of NNIs aimed at maximizing binding affinity to RT. The crystal structure of HEPT and MKC-442 complexed with RT suggested that a major determinant of increased potency in the analogues of HEPT is an improved interaction between residue Tyr181 in the protein and the 6-benzyl ring of the inhibitors, which stabilizes the structure of the complex [51]. More recently, the 2.65 Å resolution structure of the complex between HIV-1 RT and the BHAP NNI, 1-(5-methanesulfonamido-1*H*-indol-2-yl-carbonyl)-4-[3-(1-methyl-ethylamino) pyridinyl] piperazine (U-90152), allowed prediction of binding modes for related inhibitors [(alkyl-amino)piperidine-BHAPs], and changes to U-90152 were suggested, such as the addition of a 6-amino group to the pyridine ring, which may make binding more resilient to mutations in the RT [12]. In the same crystal structure, the

observation of a novel hydrogen bond between the inhibitor and the RT main chain provided clues for the improvement of quite different inhibitors. Additionally, the crystal structures of HBY-97 [*S*-4-isopropoxycarbonyl-6-methoxy-3-(methyl-thiomethyl)-3,4-dihydroquinoxalin-2(1*H*)-thione] complexed with wild-type HIV-1 RT as well as with the HIV-1 RT Y188L mutant were determined by x-ray crystallography [53]. Compared with other RT structures, considerable conformational changes to structural elements forming the NNI binding site were observed, and the loss of binding energy was partially offset by additional contacts resulting from conformational changes of the inhibitor and nearby amino acid

residues. Their observations suggested that inhibitor flexibility can help minimize drug resistance.

However, it became apparent that each reported crystal structure of an RT–NNI complex had a unique binding pattern specific to one chemical class of inhibitors. In this context, it is noteworthy that an analysis of the RT–APA structure [43] cannot be used to predict that the chemically dissimilar inhibitor TNK could bind in the same region. The RT–APA structure showed that there would not be enough room in the APA binding site for the 1-benzyl-oxymethyl group of TNK. Nevertheless, TNK is now known to bind in this region, as evidenced by the crystal structure of RT–TNK, which shows that RT residues can adjust to accommodate the 1-benzyloxymethyl group [51]. Conversely, an analysis of the RT–TNK complex does not predict favorable binding of APA in the TNK binding site. The structure does not show how residue E138 could move to accommodate the 2-acetyl group of the α-APA inhibitor. Thus, any NNI binding pocket model based on an individual RT–NNI crystal structure would have limited potential for predicting the binding of new, chemically distinct inhibitors.

In principle, *ab initio* design or derivatization of a lead compound based on the geometry of its targeted protein binding site should be possible. Since the binding site is hardly rigid, and one crystal structure may not reflect the flexible nature of the binding site, rational drug design efforts would benefit from using as many crystal structures as possible. Recent studies reported a method to combine the NNI binding site coordinates of nine RT–NNI crystal structures to generate a composite molecular surface that revealed the flexible nature of the NNI binding pocket [54–56]. This composite pocket contains features that were
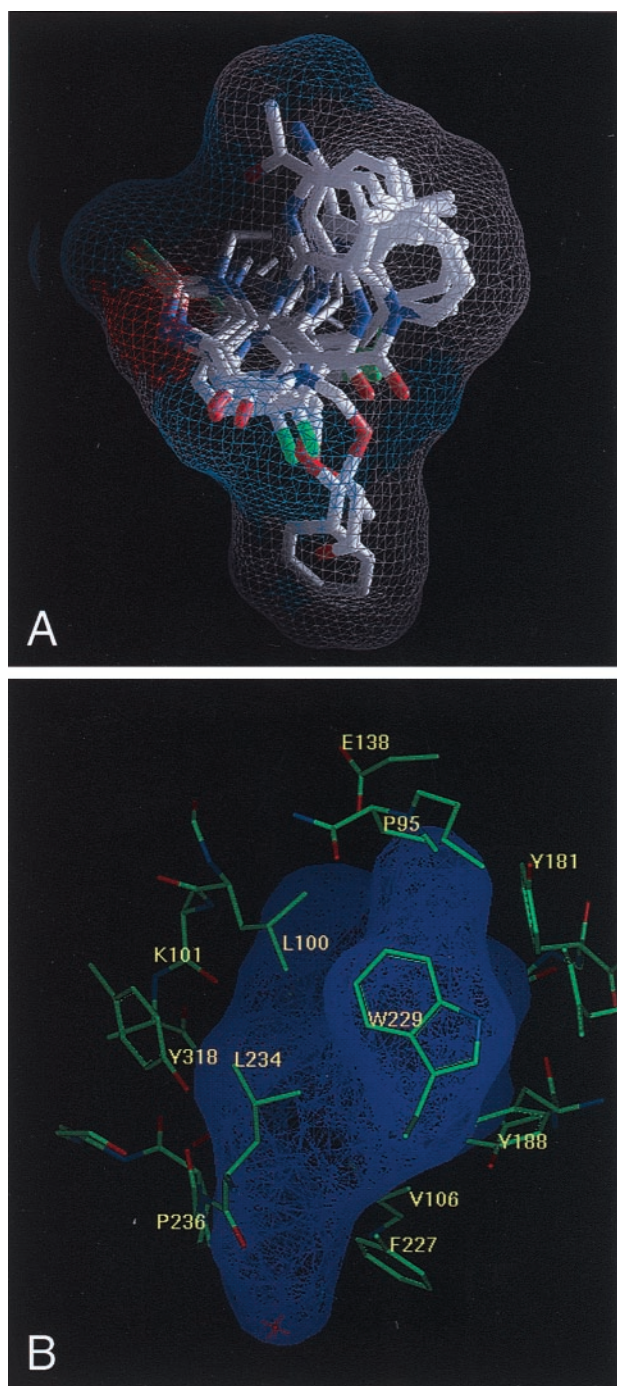
FIG. 3. (A) The composite binding pocket of the NNI binding site of HIV-1 RT. Grid lines represent the collective van der Waals surface of 9 different inhibitor crystal structures superimposed in the active site and highlight the available space for binding (inhibitor structures include HEPT, MKC, TNK, APA, nevirapine, N-ethyl nevirapine derivative, 8-Cl TIBO, and two 9-Cl TIBO compounds, with PDB access codes 1rti, 1rt1, 1rt2, 1hni, 1vrt, 1rth, 1hnv, 1rev, and 1tvr, respectively). The surface is color-coded for hydrogen bonding (orange), hydrophobic (gray), and hydrophilic (blue) groups of the superimposed inhibitors. The hydrogen atoms were not included. (B) The composite binding pocket (purple) superimposed on the active site residues of RT taken from the crystal structure coordinates of RT complexed with 8-Cl-TIBO (PDB access code: 1hnv). In the composite binding pocket, there are a number of regions that are larger than those defined by residues in individual crystal structures. Residues shown here that extend too close to or beyond the purple surface and toward the center of the binding site represent regions that are considered flexible and could be displaced by an appropriate inhibitor. Considering the limited inhibitor binding knowledge gained from individual structures, we felt that rational drug design efforts should rely on as many crystal structures as possible for maximum benefit. The composite binding pocket we present here provides a way to overcome this limitation. The composite binding pocket, which integrates structural information about the NNI binding pocket of HIV RT, can be used to design potent anti-HIV compounds that are expected to be more effective than known NNIs.
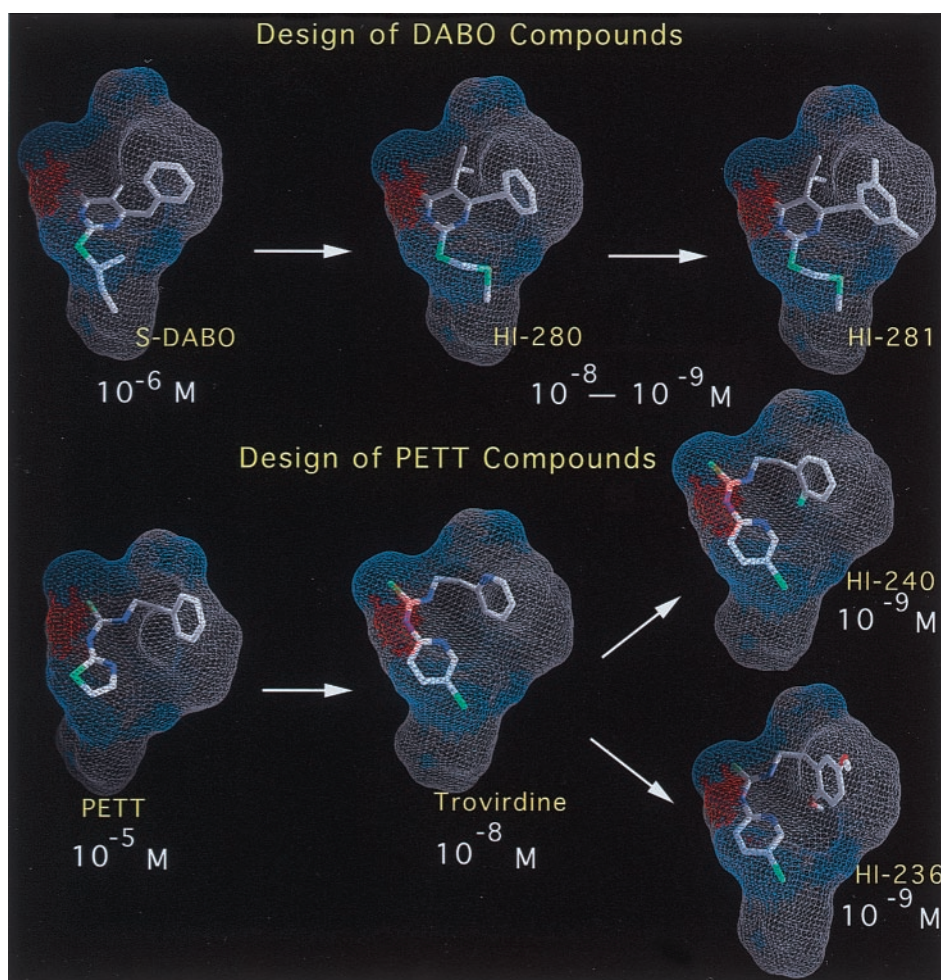
FIG. 4. Design of DABO and PETT compounds using a composite NNI binding pocket model. The IC$_{50}$ values of these compounds are shown below each compound. The surface of the composite binding pocket is color-coded for chemical preference: gray for hydrophobic regions, blue for polar regions, and red for hydrogen bonding regions.

not identified or predicted by any of the individual structures alone (Fig. 3). The composite binding pocket served as a probe to more accurately define the potentially usable, previously unrecognized space in the binding site. A number of RT residues in contact with the inhibitors are relatively flexible and vary from structure to structure. These residues include Tyr180, Tyr181, Tyr318, Tyr319, Phe227, Leu234, Trp229, Pro95, and Glu138 (Glu138 is from the p51 subunit of RT). The model also helped the implementation of information on chemical preference in the binding pocket model based on the nature of the predicted favorable interactions (hydrophilic, hydrophobic, hydrogen-bonding) to facilitate the design of new inhibitors. The surface of the binding pocket was color-coded accordingly to represent these three different regions after examining the physical nature of the known inhibitors binding to the region. The flexible nature of the residues allows them to be displaced by the right inhibitor. The resulting model (the composite binding pocket model, as shown in Fig. 3) provided an effective method for selecting favorable substituents not only by size but also by physical nature. The model predictions were consistent with *in vitro* biological assays of the anti-HIV activity of the designed and synthesized compounds (see details below). The novel composite binding pocket was utilized, together with a

computer docking procedure and a structure-based semi-empirical score function, as a guide to predict energetically favorable positions of novel derivatives in the NNI binding site of RT.

DESIGN OF POTENT NNIs (S-DABO AND PETT COMPOUNDS) BY THE COMPOSITE POCKET MODEL

S-DABO derivatives targeting the NNI binding site of HIV RT were synthesized based on the composite NNI binding pocket model [56]. The computational approach allowed the identification of several ligand derivatization sites for the generation of more potent *S*-DABO derivatives. When the lead compound, a DABO derivative, was docked into the binding pocket model, it showed significant space surrounding the 6-benzyl ring and the 5th position of the thymine ring, which led to the design and synthesis of compounds HI-280 and HI-281 (Fig. 4). The inhibition constants of these molecules were calculated based on an interaction score function. The trend of the calculated K_i values predicted that compounds having a slightly larger group at the C-5 position of the thymine ring would show stronger inhibition of RT; this general trend was also observed for the measured IC$_{50}$ values. Compound HI-280
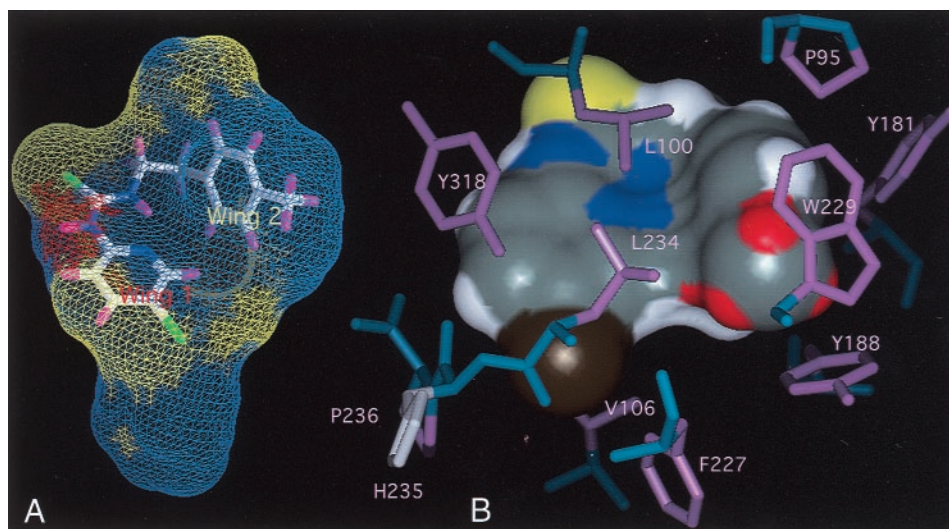
FIG. 5. (A) Composite binding pocket of the NNI binding site of HIV-1 RT is illustrated as grid lines representing the collective van der Waals surface. The surface model was constructed as previously described [54–56]. The stick model of the docked compound HI-244 in the composite NNI binding pocket is also depicted. A blue surface represents the hydrophobic region of the binding site, red is the hydrogen-bonding region, and yellow is the polar region. The *para*-methyl group of HI-244 is compatible with the hydrophobic area of the Wing 2 region. (B) Connolly surface representation of compound HI-244 in the NNI binding site. The molecular surface area associated with hydrogen atoms on the methyl group is colored in red for clarity. Nitrogen atoms are colored in blue, bromine in brown, sulfur in yellow, carbon in gray, and other hydrogens in white. The residues in contact with the compound are labeled and shown as stick models (pink for side-chains and steel-blue for main chains), prepared using InsightII [47].

elicited potent anti-HIV activity with an IC_{50} value of less than 1 nM for inhibition of HIV replication (Table 1) without any evidence of cytotoxicity and showed a selectivity index of >100,000. A similar strategy was used to study trovirdine to develop more potent compounds. When trovirdine and other PETT molecules were docked into the binding site, the composite binding pocket showed space around the phenyl ring in the Wing 2 region of the binding site. Therefore, compound HI-236 was designed and synthesized to optimize occupancy of the potentially usable space predicted by the binding pocket model of RT (Fig. 4). HI-236 elicited potent anti-HIV activity with an IC_{50} value of less than 1 nM for inhibition of HIV replication, without any evidence of cytotoxicity, and with an unprecedented selectivity index of >100,000.
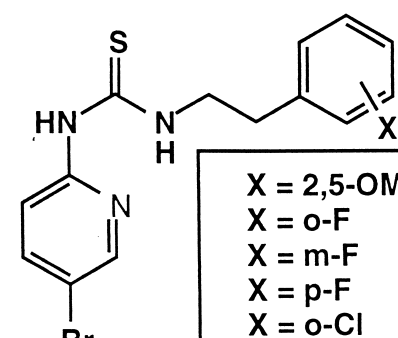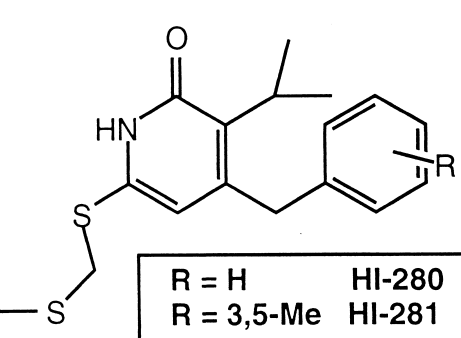
In contrast, fluoro-substituted PETT derivatives targeting HIV RT were designed using chemical preferences that were determined using the binding pocket model [55] (Fig. 4). The binding pocket was used to predict the favorable placement of chemical groups at multiple modification sites on the parent compound. The model predictions were validated by *in vitro* biological assays of the anti-HIV activity of the designed and synthesized compounds. One of the most potent compounds in this series, HI-240, abrogated HIV replication in peripheral blood mononuclear cells at nanomolar concentrations (IC_{50} < 1 nM), but showed no detectable cytotoxicity even at concentrations of 100 μM.

DRUG RESISTANCE OF MDR (V106A) MUTANT

The multiple drug-resistant strain RT-MDR carries many mutations, only one of which, V106A, is in the NNI

binding site, and which is likely to be responsible for its resistance to NNIs. The V106 residue is situated in between the Wing 1 and Wing 2 regions of the NNI binding site of RT, but is closer to Wing 1 (Figs. 1B and 2). The two terminal methyl groups of V106 are in hydrophobic contact with NNI compounds. The aromatic ring of nevirapine loses most of the van der Waals contact with V106 in the Wing 1 region of the binding pocket when V106 is mutated to an alanine. The V106 residue also provides hydrophobic contact with the middle portion of the delavirdine molecule (partly with the five-membered ring and partly with the linker group of the molecule). The loss of van der Waals contact and thus lower binding affinity with the binding pocket may explain why the MDR strain (V106A) shows considerable resistance to both nevirapine and delavirdine. An examination of how the hydrophobic contact loss may be correlated with the striking difference in resistance to *S*-DABO and PETT derivatives was proposed to aid the understanding of the structural basis of the resistance. The contribution of the van der Waals contact between the V106 residue and the *S*-DABO compounds or the PETT compounds was calculated (Table 1). These values reflected the net loss of interactions between the compounds and RT when V106 was mutated to alanine. The extent of the resistance appears to be correlated with the contact loss, although it probably is not the sole factor determining the resistance. Further analysis revealed that the extensive contact of the V106 residue with the alkylthio group of *S*-DABO provides additional van der Waals contact and therefore results in a larger loss of van der Waals contact upon mutation than for the PETT compounds. The van der Waals contact that V106 provides for the *S*-DABO com-

TABLE 1. Resistance of the MDR (V106A) strain of HIV-1 RT to inhibition by NNIs and correlation with loss of the van der Waals contact between the inhibitor and RT residues

X = 2,5-OMe HI-236
X = o-F   HI-240
X = m-F   HI-241
X = p-F   HI-242
X = o-Cl   HI-253

R = H   HI-280
R = 3,5-Me HI-281

	NNIs	WT RT IC_{50} p24 (μM)	MDR RT, IC_{50} p24 (μM)	Resistance relative to WT RT (fold)	MS loss (Å^2)
DABO	HI-280	≤ 0.001	28	~28,000	25.5
	HI-281	0.02	7	~350	24.6
PETT	HI-236	≤ 0.001	0.005	~5	19.9
	HI-253	≤ 0.001	0.004	~4	17.9
	HI-241	≤ 0.001	0.02	~20	17.7
	HI-240	≤ 0.001	0.006	~6	17.7
Reference compounds	Delavirdine	0.009	0.4	44	ND
	Nevirapine	0.034	5	147	ND
	MKC-442	0.004	0.3	75	ND
	Trovirdine	0.007	0.02	~3	ND
	AZT	0.004	0.15	~38	ND

MS = molecular surface; MS loss = decreased molecular surface contact between the inhibitor and MDR RT residues, relative to wild-type (WT) RT [57]. ND = not determined. The results are presented as IC_{50} values (i.e. concentration at which the compound inhibits RT activity by 50%). The anti-HIV activity of the compounds was measured by determining their ability to inhibit the replication of the HIV-1 strains HTLV$_{IIIB}$ and RT-MDR in PBMC from healthy volunteer donors, as described [58,59]. The results are presented as the IC_{50} values for inhibition of HIV p24 antigen production in PBMC (i.e. concentration at which the compound inhibits p24 production by 50%). A Microculture Tetrazolium Assay (MTA), using 2,3-bis(2-methoxy-4-nitro-5-sulfophenyl)-5-[(phenylamino)-carbonyl]-2H-tetrazolium hydroxide (XTT), was performed to evaluate the cytotoxicity of the compounds, as previously reported.

pounds may help position the alkylthio group in a favorable conformation, more so than for PETT derivatives. As previously reported [56], when HEPT derivatives such as MKC-442 and S-DABO derivatives are superimposed and docked into the NNI binding site of RT, the alkoxy group of MKC-442 resides in the same location as the alkylthio group of the S-DABO compound. Based on this observation and on modeling studies, MKC-442 also would be expected to lose contact with the binding site of the RT mutant to an extent similar to that predicted for S-DABO, and would show poor inhibition of the RT mutant as did the S-DABO compounds. Indeed, MKC-442 showed a 100-fold reduced inhibitory activity against the MDR mutant strain. Taken together, PETT derivatives were observed to have an inherent advantage over S-DABO compounds against the V106A mutant because PETT compounds form more favorable contacts with the binding pocket.

DRUG RESISTANCE OF RT Y181C AND Y188C MUTANTS

Score functions can be used to understand the drug resistance of the Y181C and Y188C mutants. Semi-empirical

score functions such as LUDI and others were derived based on the known crystal structure with known binding constants [60–62]. The score functions directly associate the binding constant with physical terms such as van der Waals contact, and estimation of entropy and solvent effect. Though at a developing stage, score functions provide a clear physical meaning for the molecular inhibition and thus can also be useful to understand the drug-resistance problem. However, the original LUDI function had a number of limitations. When the LUDI function was modified by taking into account unfavorable functional groups, the binding estimations became more predictable [55]. The modified function resulted in a good correlation between the predicted inhibition constants and the experimentally determined IC_{50} values for a series of NNI compounds. Based on the model (Fig. 5), the para-substituted group was located within a hydrophobic region indicated by the composite NNI binding pocket. This region contains the aromatic rings of residues W229 and Y188, which would interact favorably with a hydrophobic group. Therefore, the observed inhibition level of the para-substituted compounds against the wild-type HIV-1 was generally proportional to the hydrophobicity of the

TABLE 2. Interaction scores, calculated K_i values, and measured IC_{50} data for a series of thiourea derivatives

Compounds	R_1	MS* (Å)	BS[†] (%)	LIPO score	K_i (calc.)[‡] (μM)	IC_{50} (rRT)[§] (μM)	IC_{50} p24 (μM)
Trovirdine	Pyridyl	276	84	679	0.7	0.8	0.007
HI-275	Phenyl	274	84	672	0.8	1.3	ND[‖]
HI-244	4-Methylphenyl	294	84	724	0.25	0.1	0.007
HI-238	4-Methoxyphenyl	302	84	729	1.2	0.9	0.015
HI-243	4-Bromophenyl	295	82	708	6.3	0.9	0.07
HI-255	4-Chlorophenyl	293	81	696	4.7	2.5	ND
HI-242	4-Fluorophenyl	284	81	674	7.8	6.4	ND
HI-256	4-Hydroxylphenyl	286	82	686	104	87.7	ND
HI-231	4-Nitrophenyl	301	79	695	84	> 100	ND

The RT inhibitory activity of the compounds was tested using purified recombinant RT and the cell-free Quan-T-RT assay system (Amersham), which utilizes the scintillation proximity assay principle, as previously described in detail. The results are presented as IC_{50} values (i.e. concentration at which the compound inhibits RT activity by 50%).

* MS, molecular surface area calculated using Connolly's MS program [46]. Defined as boundary of volume within any probe sphere (meant to represent a water molecule) of given radius sharing no volume with hard sphere atoms that make up the molecule. Values are slightly smaller than those approximated by the Ludi program [61, 62].

[†] BS, buried surface: percentage of molecular surface in contact with protein calculated by Ludi based on docked positions. Based on published crystal structures of RT complexes, our calculation shows that these values could be as low as 77% (in RT–HEPT complex) and can be as high as 90% (in RT–APA complex) but most of them average around 84%.

[‡] Ludi K_i values were calculated based on modified empirical score function in the Ludi program [61, 62]. Ideal hydrogen bond distances and angles between compounds and protein are assumed in all cases for Ludi Score and K_i calculation. The number of rotatable bonds (2, or 2+n for n methoxy groups) is used in the Ludi calculation to reflect loss of binding energy due to freezing of internal degrees of freedom.

[§] rRT, recombinant HIV reverse transcriptase.

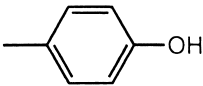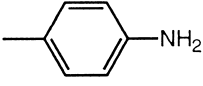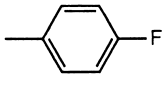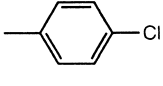[‖] ND, not determined, for compounds with IC_{50} (rRT) greater than 1.0 μM.
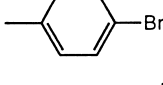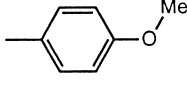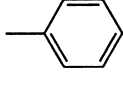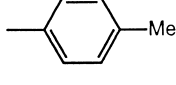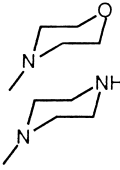
para-substituted group (Table 2). The potency of the *para*-substituted compounds was consistent with the following trend: hydrophobic group > polar group > hydrophilic group. Based on this study, the substitution of a hydrophilic functional group, such as an OH, NO_2, or SH group, near an aromatic residue typically led to a 100-fold loss in inhibition (Table 3). Consider two situations: (A) a hydrophilic functional group (e.g. SH) on the bound inhibitor is near an aromatic RT residue such as Trp229; (B) an aromatic ring of the inhibitor is near a hydrophilic thio group of a cysteine residue such as Cys181. In example A, a bound inhibitor contains a less favorable *para*-SH group, whereas in example B, an inhibitor is bound to the Y181C mutant containing an SH group. In example B, the positions of the two interacting groups (a thio group and an aromatic ring) are swapped relative to example A, and thus the interactions in both cases are similar. This is consistent with the observation that the Y181C RT mutant and the Y188C mutant are both approximately 100-fold resistant to PETT compounds. The resistance may be due in part to the presence of an aromatic ring in the PETT compounds that is predicted to bind near the mutated residue C181 or C188.
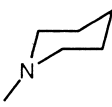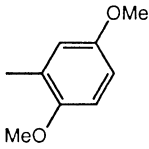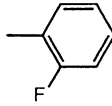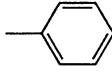
Another binding score function was developed recently

by Jain [60], who used a combination of a Gaussian-like function and a sigmoidal function to represent distances among all possible atom pairs between the inhibitor and protein residues to express entropy and hydrophobic, polar, and charge interactions. Jain's function was derived based on 34 compounds (having known inhibition constants) that were repositioned by a docking procedure. Jain's function was used to study cyclohexenyl-containing thiourea compounds (Table 4). The analysis led to the identification of HI-346 and HI-445, and also resulted in the identification of atoms in HI-347 that may be responsible for its relatively poor inhibition [63]. The docking results indicated that the cyclohexenyl group of HI-346 is situated in the Wing 2 region of the NNI binding pocket, providing contact with RT residues including Y181. The cyclohexenyl group is slightly favored over the pyridyl group of trovirdine relative to its hydrophobic interactions with RT residues. Based on the calculation, HI-346 makes 94 hydrophobic contacts with the surrounding RT residues including P95, Y181, L100, V179, and Y188, which translates into a 3.0 log unit gain in the final interaction score. The pyridyl group of the reference compound trovirdine bound to the same region of RT would make 81 contacts with surrounding residues, resulting in a 2.7 log unit gain in the
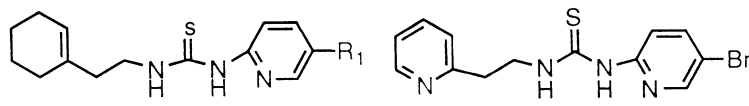
TABLE 3. Predicted effect of functional group substitutions on binding of PETT derivatives to HIV RT

Compounds	Classification of functional group R on compound	R	HIV RT residue predicted to interact with compound	HIV RT binding prediction
Aromatic PETTs	Hydrophilic	OH	Trp229	2 log fold loss
		NH₂		2 log fold loss
	Halogen	F	Trp229	1 log fold loss
		Cl	Trp229	1 log fold loss
		Br	Trp229	1 log fold loss
	Polar	O–Me	Trp229	3-fold loss
	Hydrophobic		Trp229	No loss
		Me	Trp229	No loss
Heterocyclic PETTs	Hydrophilic		Trp229	2 log fold loss
			Trp229	2 log fold loss
	Hydrophobic		Trp229	No loss
Aromatic PETTs	Hydrophobic		Tyr 181 Cys mutant	2 log fold loss

final interaction score. The alicyclic cyclohexenyl group contains more ring hydrogens than the heterocyclic pyridyl ring and therefore has more hydrogen atom-mediated contacts and fewer carbon atom-mediated contacts with RT residues than the pyridyl ring. The composite binding pocket also indicated a region in Wing 1 that would be compatible with polar atoms; this region corresponds to the predicted location of the bound halogen atoms of HI-346

TABLE 4. Interaction scores and calculated K_i values of cyclohexenyl-containing thiourea compounds (see text [55, 60])

Trovirdine

Compound	R_1	Hydrophobic score*	Polar score[†]	Solvent[‡]	Entropic[§]	K_i (µM)
HI-346	Br	10.2	1.7	−1.8	−3.3	0.16
HI-445	Cl	9.7	1.7	−1.9	−3.2	0.50
HI-347	CF$_3$	8.8	0.2	−1.6	−3.3	63
Trovirdine		10.2	0.5	−1.2	−3.3	0.63

* Hydrophobic term of Jain's score function [55].
[†] Polar term (hydrogen bond).
[‡] Solvent effect term.
[§] Entropic term.

and HI-445. The bromine atom of HI-346 makes 21 contacts with 7 RT residues including H235, L234, and V106 because of its large van der Waals radius. The estimated values for the hydrophobic score function in log units were 10.2 for HI-346 and 9.7 for HI-445, whereas the estimated value for the polar score function in log units was 1.7 for HI-346 as well as HI-445. The estimated K_i values were 0.16 µM for HI-346 and 0.50 µM for HI-445, which were better than the K_i value of 0.63 µM for trovirdine. As shown in Table 5, both HI-346 and HI-445 were more effective than trovirdine as well as the control NNI compounds nevirapine and delavirdine in inhibiting recombinant RT. Furthermore, both compounds were slightly more effective than trovirdine, as well as the control anti-HIV compounds nevirapine, delavirdine, MKC-442, and AZT, in inhibiting the replication of the NNI-sensitive/AZT-sensitive HIV-1 strain HTLV$_{IIIB}$ (Table 5). The ranking order of efficacy in cellular HIV-1 inhibition assays was as follows: HI-445 = HI-346 (IC$_{50}$ = 3 nM) > MKC-442 (IC$_{50}$ = 4 nM) = AZT (IC$_{50}$ = 4 nM) > trovirdine (IC$_{50}$ = 7 nM) > delavirdine (IC$_{50}$ = 9 nM) >

nevirapine (IC$_{50}$ = 34 nM). Jain's function may potentially be useful to further quantify NNI resistance.

DESIGN OF MORE EFFECTIVE NNI AGAINST Y181C AND K103N MUTANTS

Among the mutants resistant to NNIs, the Y181C and K103N mutants may be some of the most difficult to treat, because they are resistant to most NNI compounds that have been examined [45, 52]. Both mutants are primary selections in the presence of nevirapine and delavirdine. The K103N mutant is selected by all three inhibitors [45].

The NNI compounds evaluated in the study contain an aromatic group that interacts with the Wing 2 region of RT (Y181 or Y188, see Figs. 1 and 2) [64]. This interaction contributes to the binding affinity of NNI compounds. The π-stacking interaction with Y181 was lost in the Y181C mutant, which was resistant to inhibition by nevirapine (IC$_{50}$ > 100 µM, Table 6), delavirdine (IC$_{50}$ 50 µM, Table 6), and the *S*-DABO compound HI-281 (IC$_{50}$ 38 µM). The PETT compounds, which showed significant potency

TABLE 5. Potent anti-HIV activity of the cyclohexenyl-containing thiourea compounds HI-346 and HI-445

Compound	R_1	R_2	IC$_{50}$ rRT (µM)	IC$_{50}$ HTLV$_{IIIB}$ (µM)	IC$_{50}$ RT-MDR (V106A) (µM)	IC$_{50}$ A17 (Y181C) (µM)	IC$_{50}$ A17 variant (Y181C, K103N) (µM)	CC$_{50}$ MTA (µM)
Trovirdine	Pyridyl	Br	0.8	0.007	0.020	0.500	> 100	> 100
HI-346	Cyclohexenyl	Br	0.4	0.003	0.001	ND	18.7	> 100
HI-445	Cyclohexenyl	Cl	0.5	0.003	0.001	0.068	30.0	> 100
HI-347	Cyclohexenyl	CF$_3$	4.0	0.079	0.038	0.300	> 100	> 100
Nevirapine	NA	NA	23	0.034	5.0	> 100	> 100	10.5
Delavirdine	NA	NA	1.5	0.009	0.4	50.0	> 100	3.6
MKC-442	NA	NA	0.8	0.004	0.3	ND	ND	> 100
AZT	NA	NA	ND	0.004	0.2	0.006	0.004	> 100

The anti-HIV activity of the compounds was measured by determining their ability to inhibit the replication of the HIV-1 strains HTLV$_{IIIB}$, RT-MDR, A17, and A17 variant in PBMC from healthy volunteer donors, as described (see additional notes in Table 6). CC$_{50}$ MTA = 50% cytotoxic concentration. NA = not applicable. ND = not determined.

TABLE 6. Resistance of the Y181C and the Y181C + K103N strains of HIV RT to inhibition by NNI, relative to wild-type (WT) RT

RT inhibitors	rRT* IC$_{50}$ (μM)	WT RT IC$_{50}$ (μM)	Y181C mutant (A17)		Y181C + K103N mutant (A17 variant)	
			IC$_{50}$ p24 (μM)	Resistance relative to WT RT (fold)	IC$_{50}$ p24 (μM)	Resistance relative to WT RT (fold)
HI-236	0.1	< 0.001	0.1	> 100	11	11,000
HI-240	0.1	< 0.001	0.2	> 200	41	41,000
HI-241	0.7	< 0.001	ND[†]	ND	ND	ND
HI-253	0.7	< 0.001	ND	ND	ND	ND
HI-280	5.6	< 0.001	> 100	> 100,000	> 100	> 100,000
HI-281	7.0	0.02	38	1,850	55	2,750
HI-443	0.8	0.030	0.048	1.5	3.3	110
Delavirdine	2.3	0.009	50	5,556	38	4,222
Nevirapine	19.8	0.034	> 100	> 2,941	> 100	> 2,941
AZT	ND	0.004	0.006[‡]	1.5	0.005[‡]	1.2

The activity of HI-236 against WT and drug-resistant HIV-1 strains was confirmed in 5 independent experiments. Similarly the lack of activity of HI-280 against drug-resistant HIV-1 strains was confirmed in 3 independent experiments. The anti-HIV activities of HI-240, HI-241, HI-253, HI-280, and HI-281 against HTLV$_{IIIB}$ with WT RT have been reported previously [18, 55, 56].

* rRT, recombinant RT assay.

[†] ND, not determined.

[‡] AZT binds to a different site on RT than NNI; therefore it would be as affected by NNI binding site mutations.

against wild-type RT, still showed significant activity against the Y181C mutant even after a 100-fold decrease in activity relative to wild-type RT. The Y181C mutant altered the favorable π-stacking interaction, resulting in an unfavorable interaction between an aromatic group of the NNI and an SH group of cysteine, which led to an approximately 100-fold increase in resistance based on the modified LUDI function (see above) (Table 6). This estimation was consistent with the resistance observed for HI-240 (200-fold increase). The calculations were not consistent, however, with the ability of the Y181C mutant to have 10- to 100-fold additional resistance to S-DABO compounds and delavirdine, but less resistance to PETT compounds. This indicates that there may be other factors involved in drug resistance by RT that were not accounted for in the modeling.

How can a compound be designed that would be more effective against RT mutants? Recent studies cited an example that suggested that adding larger groups on a lead compound such as HI-240 would improve interactions with the Wing 2 region of the binding site [55]. Of course, these designs should be based on an understanding of the molecular mechanism underlying the NNI resistance. First, based on modeling studies using RT crystal structures and considering the more complete picture provided by the recently published RT/DNA/dNTP structure [35], an important factor was revealed that may contribute to the interpretation of the mechanism of NNI resistance. This involves how the binding of NNI forces RT residue W229 to change its position slightly and causes residues Y181 and Y188 to rotate into another rotamer conformation. Consequently, the binding pocket would be substantially larger than it was before NNI binding, forcing the primer–template into an inactive binding conformation and rendering the protein inactive [35]. The volume change is a direct consequence of

the different positions of the Y181, Y188, and W229 side-chains before and after the NNI binding. When Y181 and Y188 were mutated to cysteine residues, the volume change due to NNI binding was smaller, and the impact of NNI inhibiting the RT mutants therefore would be attenuated. Hence, a compound that has a maximum occupancy at the Wing 2 region most likely will have an advantage against Wing 2 mutants, such as the Y181C and Y188C mutants. In summary, based on the resistance data, it is hypothesized that an ideal NNI compound that (a) is highly potent against wild-type RT and therefore can afford a considerable activity loss against mutants (i.e. a picomolar-level inhibitor against wild-type RT may still be effective against RT mutants at nanomolar concentrations), and (b) maximizes the occupancy at the Wing 2 region, will most likely have an advantage against the Wing 2 mutants, such as the especially problematic Y181C RT mutant. This theory adds another strategy to a recent finding that a flexible functional group at the Wing 2 region may result in NNI compounds more potent against the Y181 mutant of RT [53].

Based on the composite binding pocket model, it was recognized previously that the Wing 2 region had a substantial molecular volume (approximately 160 Å^3) surrounding the phenyl ring at the Wing 2 region, defining space that potentially can be occupied more efficiently by a larger functional group [54]. Next, a thiourea compound with optimized van der Waals contact with the binding pocket was examined. This strategy was predicted to improve the potency against wild-type RT and the inhibition profile against Wing 2 mutants of RT. The compound HI-236, which contains one methoxy group at the 2′ position (the same position as the fluoro atom of HI-240) and another methoxy group at the 5′ position of the phenyl ring, can contact the Wing 2 region better than HI-240. Docking results showed that the unoccupied volume sur-

rounding HI-236 in the NNI binding site of RT was 135 $Å^3$, a decrease of 25 $Å^3$ relative to the unoccupied volume surrounding HI-240 (160 $Å^3$). These docking results were consistent with activity data showing an improved potency for HI-236, which can contact RT residues better than HI-240 (Table 6). HI-236 was predicted to have a better K_i value than trovirdine against the RT mutants because it contained a larger functional group, which had more contact with the Wing 2 region of RT when Y181 or Y188 of RT was mutated to a smaller residue, Cys. HI-236 demonstrated an IC_{50} value of 0.005 μM against MDR RT (slightly better than that for HI-240), 0.1 μM against the Y181C mutant (two times better than that for HI-240), and 11 μM against Y181C + K103N (four times better than that for HI-240). These results were consistent with predictions that HI-236 would be a more potent anti-HIV compound than HI-240. Compounds HI-236 and HI-240 were 100–200 times less active against the Y181C RT mutant relative to wild-type RT (Table 6), yet maintained a useful activity level (IC_{50} values of 0.1 μM and 0.2 μM, respectively).

Both alterations in the Y181C and Y188C mutants demonstrate a dramatic change from a hydrophobic environment to a hydrophilic environment. It is, therefore, difficult for any functional groups binding in the affected region to be totally compatible with two totally different binding situations. However, there must exist such a functional group that has a good balance between its inhibition against wild-type RT and mutant RT—a small loss in potency against wild-type RT is compensated for by a considerable gain of inhibition against mutant RT. The designed compound HI-443, which contains a thiophene group predicted to bind at the Wing 2 region, may demonstrate such a successful strategy [65]. When the thiophene-containing thiourea compound HI-443 was modeled into the NNI binding site of RT using a docking procedure, the location of the thiophene group of HI-443 was in close proximity to the Y181 residue. In this docked position, the sulfur atom of the thiophene ring was only 4.4 Å away from the C(γ) atom of the tyrosine 181 residue, which was mutated to a sulfur atom in the RT Y181C mutant strains (A17 or A17 variant). Therefore, in the Y181C mutant, while the thiophene ring loses hydrophobic contact with the side-chain atoms of residue 181, the sulfur atom of the thiophene group may be more compatible with the sulfur-containing cysteine 181 residue, relative to tyrosine 181 in wild-type RT. HI-443 effectively inhibited the replication of the HIV-1 strain HTLV$_{IIIB}$ in human PBMC with an IC_{50} of 0.03 μM (Table 6). Surprisingly, HI-443 was 10 times more effective against the multidrug-resistant HIV-1 strain RT-MDR with a V106A mutation as well as additional mutations involving RT residues 74V, 41L, and 215Y, relative to its activity against the HTLV$_{IIIB}$ strain containing wild-type RT. HI-443 was 5 times more potent than trovirdine, 1250 times more potent than nevirapine, 100 times more potent than delavirdine, 75 times more potent than MKC-442, and 50 times more

potent than AZT against the multidrug-resistant HIV-1 strain RT-MDR. HI-443 was almost as potent against the NNI-resistant HIV-1 strain A17 with a Y181C mutation relative to HTLV$_{IIIB}$ (IC_{50} 0.048 vs 0.030 μM). The activity of HI-443 against A17 was 10 times more potent than that of trovirdine, 2083 times more potent than that of nevirapine, and 1042 times more potent than that of delavirdine. HI-443 inhibited the replication of the NNI-resistant HIV-1 strain A17 variant containing the Y181C plus K103N RT mutations and had an IC_{50} of 3.263 μM, whereas the IC_{50} values of trovirdine, nevirapine, and delavirdine were all at least ten times worse. These findings established the novel thiophene-containing thiourea compound HI-443 as an NNI with potent antiviral activity against NNI-sensitive, NNI-resistant, and multidrug-resistant strains of HIV-1 [65].

CONCLUSIONS

Several different NNIs of HIV RT have been developed in recent years using structure-based methods, which included crystallographic analysis of RT–inhibitor complexes as well as a classical evaluation of structure–activity relationships. An emerging concern, however, is how useful these potent agents will be against drug-resistant strains of HIV RT. To combat the problem of drug-resistant RT mutants, a recent study was undertaken that used molecular modeling to design agents that may be more effective. The result was a new generation of NNIs, which were identified using a novel structure-based method that utilized a model of the NNI binding site of HIV RT. This model, termed the composite binding pocket, integrated all available crystal structure information about the NNI binding site of HIV RT. The model was demonstrated to be an effective tool to better comprehend the flexible nature of the binding pocket and to identify specific areas for structural improvements of the inhibitors. In addition, we developed a modeling procedure to better understand the drug-resistance mechanism and to develop high-potency NNI. Based on these studies, several potent PETT compounds, HI-236, HI-240, HI-244, HI-253, HI-443, and HI-445, were identified, which were active against both wild-type HIV RT and drug-resistant mutants of RT.

Further analysis prompted the hypothesis that for an NNI of HIV RT to be active against NNI-resistant strains containing mutants in the Wing 2 region of the binding site (e.g. the especially problematic Y181C RT mutant), the inhibitor should optimize the following features: (a) the inhibitor should be highly potent against wild-type RT and therefore be able to afford a considerable activity loss against mutants, (b) the inhibitor should maximize the occupancy in the Wing 2 region of the NNI binding site of RT, and (c) the inhibitor should contain functional groups that provide a good balance of favorable chemical interactions with Wing 2 residues of RT as well as RT mutants. The compounds that combined these desired elements outperformed other anti-HIV agents tested.

References

1. Greene WC, The molecular biology of human immunodeficiency virus type 1 infections. *N Engl J Med* **324:** 308–317, 1991.

2. De Clercq E, HIV inhibitors targeted at the reverse transcriptase. *AIDS Res Hum Retroviruses* **8:** 119–134, 1992.

3. Mitsuya H, Yarchoan R and Broder S, Molecular targets for AIDS therapy. *Science* **249:** 1533–1544, 1990.

4. Satcher D, Gayle HD, De Cock KM, Ward JM, Fleming PL, Metler PR and Santas XM, HIV/AIDS Surveillance Report. U.S. HIV and AIDS cases reported through June 1997. *Hiv/Aids Surveill Rep* **9:** 1–37, 1997.

5. Goldschmidt RH and Dong BJ, Treatment of AIDS and HIV-related conditions—1997. *J Am Board Fam Pract* **10:** 144–167, 1997.

6. Deeks SG and Volberding PA, HIV-1 protease inhibitors. *AIDS Clin Rev* 145–185, 1997–98.

7. Miles SA, HIV infection and AIDS: New biology, therapeutic advances, and clinical implications. Introduction. *J Acquir Immune Defic Syndr* **16** (Suppl 1): S1–S2, 1997.

8. Havlir DV and Richman DD, Viral dynamics of HIV: Implications for drug development and therapeutic strategies. *Ann Intern Med* **124:** 984–994, 1996.

9. Grob PM, Wu JC, Cohen KA, Ingraham RH, Shih CK, Hargrave KD, McTague TL and Merluzzi VJ, Nonnucleoside inhibitors of HIV-1 reverse transcriptase: Nevirapine as a prototype drug. *AIDS Res Hum Retroviruses* **8:** 145–152, 1992.

10. Romero DL, Morge RA, Genin MJ, Biles C, Busso M, Resnick L, Althaus IW, Reusser F, Thomas RC and Tarpley WG, Bis(heteroaryl)piperazine (BHAP) reverse transcriptase inhibitors: Structure–activity relationships of novel substituted indole analogues and the identification of 1-[(5-methanesulfonamido-1*H*-indol-2-yl)-carbonyl]-4-[3- [(1-methylethyl)amino]-pyridinyl]piperazine monomethanesulfonate (U-90152S), a second-generation clinical candidate. *J Med Chem* **36:** 1505–1508, 1993.

11. Romero DL, Olmsted RA, Poel TJ, Morge RA, Biles C, Keiser BJ, Kopta LA, Friis JM, Hosley JD, Stefanski KJ, Wishka DG, Evans DB, Morris J, Stehle RG, Sharma SK, Yagi Y, Voorman RL, Adams WJ, Tarpley WG and Thomas RC, Targeting delavirdine/atevirdine resistant HIV-1: Identification of (alkylamino)piperidine-containing bis(heteroaryl)piperazines as broad spectrum HIV-1 reverse transcriptase inhibitors. *J Med Chem* **39:** 3769–3789, 1996.

12. Esnouf RM, Ren J, Hopkins AL, Ross CK, Jones EY, Stammers DK and Stuart DI, Unique features in the structure of the complex between HIV-1 reverse transcriptase and the bis(heteroaryl)piperazine (BHAP) U-90152 explain resistance mutations for this nonnucleoside inhibitor. *Proc Natl Acad Sci USA* **94:** 3984–3989, 1997.

13. Young SD, Britcher SF, Tran LO, Payne LS, Lumma WC, Lyle TA, Huff JR, Anderson PS, Olsen DB, Carroll SS, Pettibone DJ, O'Brien JA, Ball RG, Balani SK, Lin JH, Chen I-W, Schleif WA, Sardana VV, Long WJ, Byrnes VW and Emini EA, L-743,726 (DMP-266): a novel, highly potent nonnucleoside inhibitor of the human immunodeficiency virus type 1 reverse transcriptase. *Antimicrob Agents Chemother* **39:** 2602–2605, 1995.

14. Danel K, Pedersen EB and Nielsen C, Synthesis and anti-HIV-1 activity of novel 2,3-dihydro-7*H*-thiazolo[3,2-*a*]pyrimidin-7-ones. *J Med Chem* **41:** 191–198, 1998.

15. Danel K, Nielsen C and Pedersen EB, Anti-HIV active naphthyl analogues of HEPT and DABO. *Acta Chem Scand* **51**(Suppl 3): 426–430, 1997.

16. Danel K, Larsen E, Pedersen EB, Vestergaard BF and Nielsen C, Synthesis and potent anti-HIV-1 activity of novel 6-benzyluracil analogues of 1-[(2-hydroxyethoxy)methyl]-6-(phenylthio)thymine. *J Med Chem* **39:** 2427–2431, 1996.

17. Mai A, Artico M, Sbardella G, Quartarone S, Massa S, Loi AG, De Montis A, Scintu F, Putzolu M and La Colla P, Dihydro(alkylthio)(naphthylmethyl)oxopyrimidines: Novel non-nucleoside reverse transcriptase inhibitors of the S-DABO series. *J Med Chem* **40:** 1447–1454, 1997.

18. Vig R, Mao C, Venkatachalam TK, Tuel-Ahlgren L, Sudbeck EA and Uckun FM, 5-Alkyl-2-[(methylthiomethyl)thio]-6-(benzyl)-pyrimidin-4-(1H)-ones as potent non-nucleoside reverse transcriptase inhibitors of S-DABO series. *Bioorg Med Chem Lett* **8:** 1461–1466, 1998.

19. Tanaka H, Baba M, Hayakawa H, Sakamaki T, Miyasaka T, Ubasawa M, Takashima H, Sekiya K, Nitta I, Shigeta S, Walker RT, Balzarini J and De Clercq E, A new class of HIV-1-specific 6-substituted acyclouridine derivatives: Synthesis and anti-HIV-1 activity of 5- or 6-substituted analogues of 1-[(2-hydroxyethoxy)methyl]-6-(phenylthio)thymine (HEPT). *J Med Chem* **34:** 349–357, 1991.

20. Pontikis R, Benhida R, Aubertin AM, Grierson DS and Monneret C, Synthesis and anti-HIV activity of novel N-1 side chain-modified analogs of 1-[(2-hydroxyethoxy)methyl]-6-(phenylthio)thymine (HEPT). *J Med Chem* **40:** 1845–1854, 1997.

21. Baba M, Shigeta S, Tanaka H, Miyasaka T, Ubasawa M, Umezu K, Walker RT, Pauwels R and De Clercq E, Highly potent and selective inhibition of HIV-1 replication by 6-phenylthiouracil derivatives. *Antiviral Res* **17:** 245–264, 1992.

22. Ding J, Das K, Moereels H, Koymans L, Andries K, Janssen PA, Hughes SH and Arnold E, Structure of HIV-1 RT/TIBO R 86183 complex reveals similarity in the binding of diverse nonnucleoside inhibitors. *Nat Struct Biol* **2:** 407–415, 1995.

23. Balzarini J, Pérez-Pérez M-J, San-Félix A, Schols D, Perno C-F, Vandamme A-M, Camarasa M-J and De Clercq E, 2′,5′-Bis-O-(*tert*-butyldimethylsilyl)-3′-spiro-5″-(4″-amino-1″,2″-oxathiole-2″,2″-dioxide)pyrimidine (TSAO) nucleoside analogues: Highly selective inhibitors of human immunodeficiency virus type 1 that are targeted at the viral reverse transcriptase. *Proc Natl Acad Sci USA* **89:** 4392–4396, 1992.

24. Balzarini J, Novel concepts in the treatment of human immunodeficiency virus type 1 (HIV-1) infections by HIV-1-specific reverse transcriptase inhibitors. *Verh K Acad Geneeskd Belg* **57:** 575–600, 1995.

25. Buckheit JRW, Kinjerski TL, Fliakas-Boltz V, Russell JD, Stup TL, Pallansch LA, Brouwer WG, Dao DC, Harrison WA, Schultz RJ, Bader JP and Yang SS, Structure-activity and cross-resistance evaluations of a series of human immunodeficiency virus type-1-specific compounds related to oxathiin carboxanilide. *Antimicrob Agents Chemother* **39:** 2718–2727, 1995.

26. Buckheit RW Jr, Snow MJ, Fliakas-Boltz V, Kinjerski TL, Russell JD, Pallansch LA, Brouwer WG and Yang SS, Highly potent oxathiin carboxanilide derivatives with efficacy against nonnucleoside reverse transcriptase inhibitor-resistant human immunodeficiency virus isolates. *Antimicrob Agents Chemother* **41:** 831–837, 1997.

27. Buckheit RW Jr, Hollingshead M, Stinson S, Fliakas-Boltz V, Pallansch LA, Roberson J, Decker W, Elder C, Borgel S, Bonomi C, Shores R, Siford T, Malspeis L and Bader JP, Efficacy, pharmacokinetics, and *in vivo* antiviral activity of UC781, a highly potent, orally bioavailable nonnucleoside reverse transcriptase inhibitor of HIV type 1. *AIDS Res Hum Retroviruses* **13:** 789–796, 1997.

28. Font M, Monge A, Alvarez E, Cuartero A, Losa MJ, Fidalgo MJ, SanMartin C, Nadal E, Ruiz I, Merino I, Martinez-Irujo JJ, Alberdi E, Santiago E, Prieto I, Lasarte JJ, Sarobe P and Borras F, Synthesis and evaluation of new Reissert analogs as HIV-1 reverse transcriptase inhibitors. 1. Quinoline and quinoxaline derivatives. *Drug Des Disc* **14:** 305–332, 1997.

29. Kleim JP, Rosner M, Winkler I, Paessens A, Kirsch R, Hsiou Y, Arnold E and Riess G, Selective pressure of a quinoxaline nonnucleoside inhibitor of human immunodeficiency virus type 1 (HIV-1) reverse transcriptase (RT) on HIV-1 replication results in the emergence of nucleoside RT-inhibitor-specific (RT Leu-74→Val or Ile and Val-75→Leu or Ile) HIV-1 mutants. *Proc Natl Acad Sci USA* **93:** 34–38, 1996.

30. Fujiwara M, Ijichi K, Hanasaki Y, Ide T, Katsuura K, Takayama H, Aimi N, Shigeta S, Konno K, Yokota T and Baba M, Thiadiazole derivatives: Highly potent and selective inhibitors of human immunodeficiency virus type 1 (HIV-1) replications *in vitro*. *Microbiol Immunol* **41:** 301–308, 1997.

31. Bell FW, Cantrell AS, Hogberg M, Jaskunas SR, Johansson NG, Jordan CL, Kinnick MD, Lind P, Morin JM Jr, Noreen R, Oberg B, Palkowitz JA, Parrish CA, Pranc P, Sahlberg C, Ternansky RT, Vasileff RT, Vrang L, West SJ, Zhang H and Zhou XX, Phenethylthiazolethiourea (PETT) compounds, a new class of HIV-1 reverse transcriptase inhibitors. 1. Synthesis and basic structure-activity relationship studies of PETT analogs. *J Med Chem* **38:** 4929–4936, 1995.

32. Cantrell AS, Engelhardt P, Hogberg M, Jaskunas SR, Johansson NG, Jordan CL, Kangasmetsa J, Kinnick MD, Lind P, Morin JM Jr, Muesing MA, Noreen R, Oberg B, Pranc P, Sahlberg C, Ternansky RJ, Vasileff RT, Vrang L, West SJ and Zhang H, Phenethylthiazolylthiourea (PETT) compounds as a new class of HIV-1 reverse transcriptase inhibitors. 2. Synthesis and further structure-activity relationship studies of PETT analogs. *J Med Chem* **39:** 4261–4274, 1996.

33. Ahgren C, Backro K, Bell FW, Cantrell AS, Clemens M, Colacino JM, Deeter JB, Engelhardt JA, Hogberg M, Jaskunas SR, Johansson NG, Jordan CL, Kasher JS, Kinnick MD, Lind P, Lopez C, Morin JMJ, Muesing MA, Noreen R, Oberg B, Paget CJ, Palkowitz JA, Parrish CA, Pranc P, Rippy MK, Rydergard C, Sahlberg C, Swanson S, Ternansky RJ, Unge T, Vasileff RT, Vrang L, West SJ, Zhang H and Zhou XX, The PETT series, a new class of potent nonnucleoside inhibitors of human immunodeficiency virus type 1 reverse transcriptase. *Antimicrob Agents Chemother* **39:** 1329–1335, 1995.

34. Heinisch G, Matuszczak B, Pachler S and Rakowitz D, The inhibitory activity of diazinyl-substituted thiourea derivatives on human immunodeficiency virus type 1 reverse transcriptase. *Antiviral Chem Chemother* **8:** 443–446, 1997.

35. Huang H, Chopra R, Verdine GL and Harrison SC, Structure of a covalently trapped catalytic complex of HIV-1 reverse transcriptase: Implications for drug resistance. *Science* **282:** 1669–1675, 1998.

36. Joyce CM and Steitz TA, Function and structure relationships in DNA polymerases. *Annu Rev Biochem* **63:** 777–822, 1994.

37. Joyce CM and Steitz TA, Polymerase structures and function: Variations on a theme? *J Bacteriol* **177:** 6321–6329, 1995.

38. Steitz TA, Smerdon SJ, Jager J and Joyce CM, A unified polymerase mechanism for nonhomologous DNA and RNA polymerases. *Science* **266:** 2022–2025, 1994.

39. Brautigam CA and Steitz TA, Structural and functional insights provided by crystal structures of DNA polymerases and their substrate complexes. *Curr Opin Struct Biol* **8:** 54–63, 1998.

40. Kohlstaedt LA, Wang J, Friedman JM, Rice PA and Steitz TA, Crystal structure at 3.5 Å resolution of HIV-1 reverse transcriptase complexed with an inhibitor. *Science* **256:** 1783–1790, 1992.

41. Smerdon SJ, Jager J, Wang J, Kohlstaedt LA, Chirino AJ, Friedman JM, Rice PA and Steitz TA, Structure of the binding site for nonnucleoside inhibitors of the reverse transcriptase of human immunodeficiency virus type 1. *Proc Natl Acad Sci USA* **91:** 3911–3915, 1994.

42. Ren J, Esnouf R, Garman E, Somers D, Ross C, Kirby I, Keeling J, Darby G, Jones Y, Stuart D and Stammers D, High resolution structures of HIV-1 RT from four RT-inhibitor complexes. *Nat Struct Biol* **2:** 293–302, 1995.

43. Ding J, Das K, Tantillo C, Zhang W, Clark AD Jr, Jessen S, Lu X, Hsiou Y, Jacobo-Molina A, Andries K, Pauwels R, Moereels H, Koymans L, Janssen PAJ, Smith RHJ, Kroeger Koepke R, Michejda CJ, Hughes SH and Arnold E, Structure of HIV-1 reverse transcriptase in a complex with the non-nucleoside inhibitor α-APA R 95845 at 2.8 Å resolution. *Structure* **3:** 365–379, 1995.

44. Ren J, Esnouf R, Hopkins A, Ross C, Jones Y, Stammers D and Stuart D, The structure of HIV-1 reverse transcriptase complexed with 9-chloro-TIBO: Lessons for inhibitor design. *Structure* **3:** 915–926, 1995.

45. Hirsch MS, Conway B, D'Aquila RT, Johnson VA, Brun-Vézinet F, Clotet B, Demeter LM, Hammer SM, Jacobsen DM, Kuritzkes DR, Loveday C, Mellors JW, Vella S and Richman DD for the International AIDS Society—USA Panel, Antiretroviral drug resistance testing in adults with HIV infection: Implications for clinical management. *JAMA* **279:** 1984–1991, 1998.

46. Connolly ML, Solvent-accessible surfaces of proteins and nucleic acids. *Science* **221:** 709–713, 1983.

47. InsightII, Molecular Simulations Inc., San Diego, CA, 1996.

48. De Clercq E, Toward improved anti-HIV chemotherapy: Therapeutic strategies for intervention with HIV infections. *J Med Chem* **38:** 2491–2517, 1995.

49. De Clercq E, The role of non-nucleoside reverse transcriptase inhibitors (NNRTIs) in the therapy of HIV-1 infection. *Antiviral Res* **38:** 153–179, 1998.

50. De Clercq E, Perspectives of non-nucleoside reverse transcriptase inhibitors (NNRTIs) in the therapy of HIV-1 infection. *Farmaco* **54:** 26–45, 1999.

51. Hopkins AL, Ren J, Esnouf RM, Willcox BE, Jones EY, Ross C, Miyasaka T, Walker RT, Tanaka H, Stammers DK and Stuart DI, Complexes of HIV-1 reverse transcriptase with inhibitors of the HEPT series reveal conformational changes relevant to the design of potent non-nucleoside inhibitors. *J Med Chem* **39:** 1589–1600, 1996.

52. Tantillo C, Ding J, Jacobo-Molina A, Nanni RG, Boyer PL, Hughes SH, Pauwels R, Andries K, Janssen PA and Arnold E, Locations of anti-AIDS drug binding sites and resistance mutations in the three-dimensional structure of HIV-1 reverse transcriptase. Implications for mechanisms of drug inhibition and resistance. *J Mol Biol* **243:** 369–387, 1994.

53. Hsiou Y, Das K, Ding J, Clark AD Jr, Kleim J-P, Rösner M, Winkler I, Riess G, Hughes SH and Arnold E, Structures of Tyr188Leu mutant and wild-type HIV-1 reverse transcriptase complexed with the non-nucleoside inhibitor HBY 097: Inhibitor flexibility is a useful design feature for reducing drug resistance. *J Mol Biol* **284:** 313–323, 1998.

54. Mao C, Vig R, Venkatachalam TK, Sudbeck EA and Uckun FM, Structure-based design of N-[2-(1-piperidinylethyl)]-N′-[2-(5-bromopyridyl)]-thiourea and N-[2-(1-piperazinyl-ethyl)]-N′-[2-(5-bromopyridyl)]-thiourea as potent non-nucleoside inhibitors of HIV-1 reverse transcriptase. *Bioorg Med Chem Lett* **8:** 2213–2218, 1998.

55. Vig R, Mao C, Venkatachalam TK, Tuel-Ahlgren L, Sudbeck EA and Uckun FM, Rational design and synthesis of phenethyl-5-bromopyridyl thiourea derivatives as potent non-nucleoside inhibitors of HIV reverse transcriptase. *Bioorg Med Chem* **6:** 1789–1797, 1998.

56. Sudbeck EA, Mao C, Vig R, Venkatachalam TK, Tuel-Ahlgren L and Uckun FM, Structure-based design of novel dihydroalkoxybenzyloxopyrimidine derivatives as potent non-nucleoside inhibitors of the human immunodeficiency virus reverse transcriptase. *Antimicrob Agents Chemother* **42:** 3225–3233, 1998.

57. Mao C, Sudbeck EA, Venkatachalam TK and Uckun FM,

Rational design of N-[2-(2,5-dimethoxyphenylethyl)]-N′-[2-(5-bromopyridyl)]-thiourea (HI-236) as a potent non-nucleoside inhibitor of drug-resistant human immunodeficiency virus. *Bioorg Med Chem Lett* **9:** 1593–1598, 1999.

58. Uckun FM, Chelstrom LM, Tuel-Ahlgren L, Dibirdik I, Irvin JD, Chandan-Langlie M and Myers DE, TXU (anti-CD7)-pokeweed antiviral protein as a potent inhibitor of human immunodeficiency virus. *Antimicrob Agents Chemother* **42:** 383–388, 1998.

59. Zarling JM, Moran PA, Haffar O, Sias J, Richman DD, Spina CA, Myers DE, Kuebelbeck V, Ledbetter JA and Uckun FM, Inhibition of HIV replication by pokeweed antiviral protein targeted to CD4$^+$ cells by monoclonal antibodies. *Nature* **347:** 92–95, 1990.

60. Jain AN, Scoring noncovalent protein-ligand interactions: A continuous differentiable function tuned to compute binding affinities. *J Comput Aided Mol Des* **10:** 427–440, 1996.

61. Bohm HJ, LUDI, rule-based automatic design of new substituents for enzyme inhibitor leads. *J Comput Aided Mol Des* **6:** 593–606, 1992.

62. Bohm HJ, The development of a simple empirical scoring function to estimate the binding constant for a protein-ligand complex of known three-dimensional structure. *J Comput Aided Mol Des* **8:** 243–256, 1994.

63. Uckun FM, Mao C, Pendergrass S, Maher D, Zhu D, Tuel-Ahlgren L and Venkatachalam TK, N-[2-(1-cyclohexenyl)ethyl]-N′-[2-(5-bromopyridyl)]-thiourea and N′-[2-(1-cyclohexenyl)ethyl]-N′-[2-(5-chloropyridyl)]-thiourea as potent inhibitors of multidrug-resistant human immunodeficiency virus-1. *Bioorg Med Chem Lett* **9:** 2721–2726, 1999.

64. Kroeger Smith MB, Rouzer CA, Taneyhill LA, Smith NA, Hughes SH, Boyer PL, Janssen PA, Moereels H, Koymans L, Arnold E, Ding J, Das K, Zhang W, Michejda CJ and Smith RH, Molecular modeling studies of HIV-1 reverse transcriptase nonnucleoside inhibitors: Total energy of complexation as a predictor of drug placement and activity. *Prot Sci* **4:** 2203–2222, 1995.

65. Uckun FM, Pendergrass S, Maher D, Zhu D, Tuel-Ahlgren L, Mao C and Venkatachalam TK, N-[2-(2-Thiophene) ethyl]-N′-[2-(5-bromopyridyl)] thiourea as a potent inhibitor of NNI-resistant and multidrug-resistant human immunodeficiency virus-1. *Bioorg Med Chem Lett* **9:** 3411–3416, 1999.